DOI https: //doi. org/10.1007/s11595-023-2670-3

# Chloride Corrosion of Reinforced Calcium Aluminate Cement Mortar

**CHEN Yuting[1], WU Kai[1*], XU Linglin[1*], WANG Zhongping[1], ZHAO Yating[1,2], ZHU Zheyu[1]**

*(1. Key Laboratory of Advanced Civil Engineering Materials of Ministry of Education, School of Materials Science and Engineering, Tongji University, Shanghai 201804, China; 2. Henan Provincial Communications Planning & Design Institute Co., Ltd, Zhengzhou 450052, China)*

**Abstract:** This paper describes a study on the corrosion behavior of steel reinforcement in CAC mortars via electrochemical methods including corrosion potential, electrochemical impedance, and linear polarization evaluation. Results indicate that there is a non-linear relationship between the corrosion degree of steel reinforcement in CAC mortar and the concentration of NaCl solution. The electrochemical parameters of specimens immersed in 3% NaCl solution suddenly drop at 40 days, earlier than 60 days of the reference. And the charge transfer resistivity of the specimen has decreased by 11 orders of magnitude at 40 days, showing an evident corrosion on steel reinforcement. However, it is interesting to notice that the corrosion is delayed by high external chloride concentration. The specimens immersed in 9% and 15% NaCl solutions remain in a relatively stable state within 120 days with slight pitting. The great corrosion protection of CAC concrete to embedded steel bars enables its wide application in marine.

**Key words:** electrochemical impedance; calcium aluminate cement mortar; chloride corrosion

## 1 Introduction

Corrosion of steel reinforcement seriously threatens the durability of reinforced concrete structures, and brings huge economic losses[1]. Generally, the pH of Portland cement concrete is maintained around 12.5-14[2-4], and in such a strong alkaline environment, a layer of the ferric oxide film can spontaneously form on the surface of steel reinforcement to ensure it is in a passive state. However, when the reinforced concrete structure is affected by carbonization and chloride attack[1,5,6], it may damage the passive film and result in the corrosion of inner steel reinforcement. Natural carbonation takes place at a relatively slow rate[7,8], only playing an important role in the corrosion of steel reinforcement when the concrete layer is not thick or porous in practical engineering[9,10]. Compared with carbonization, the corrosion caused by chloride permeation is more serious. The external chloride ions can easily permeate into the concrete structure and compete with the hydroxide ions in the pore solution to adsorb on the surface of steel reinforcement[11,12]. On one hand, the adsorbed chlorides cause shrinkage, cracking, and even completely destroying of passive film[1]. On the other hand, it leads to the decrease of local pH at the interface between steel reinforcement and concrete matrix, accelerating the ionization process of iron, as shown in Eqs.(1) and (2)[1]. Moreover, the deposition of corrosion oxides (Eqs.(3) - (5)) on the surface of steel reinforcement can result in high expansion stress, which further leads to the cracking of the whole concrete structure[1,13].

Anode reaction:

$$Fe \rightarrow Fe^{2+}+2e^{-} \quad (1)$$

Cathodic reaction:

$$2H_2O+O_2+4e^{-} \rightarrow 4OH^{-} \quad (2)$$

Further oxidation of ferrous ions:

$$Fe^{2+}+2OH^{-} \rightarrow Fe(OH)_2 \quad (3)$$

$$4Fe(OH)_2+2H_2O+O_2 \rightarrow 4Fe(OH)_3 \quad (4)$$



(Received: June 26, 2022; Accepted: Sept. 18, 2022)

CHEN Yuting (陈钰婷) : Ph D; E-mail: chen15901737773@126.com

*Corresponding author: WU Kai (吴凯): Assoc. Prof.; Ph D; E-mail: wukai@tongji.edu.cn; Xu Linglin (徐玲琳): Assoc. Prof.; Ph D; E-mail: xulinglin@126.com

Funded by National Natural Science Foundation of China (Nos. 51772212, 51402216, 51978505)

$$2Fe(OH)_3 \rightarrow Fe_2O_3 \cdot H_2O + 2H_2O \quad (5)$$

In view of the above-mentioned steel corrosion in Portland cement concrete, the most important prevention method at present is using corrosion inhibitors[14-18]. However, the performances of commercially available corrosion inhibitors are uneven and there are compatibility problems with concrete matrix[19-21], which easily leads to poor durability in practical application. Based on this, the durability issues and performance improvement of reinforced concrete structures give impetus to the development of new types of cementitious materials[22,23]. Due to the different hydration mechanism and the composition of pastes, more and more attention needs to be paid to the impact of new cementitious materials on the long-term performance and protection of steel bars. For instance, many studies investigated the chloride permeability and corrosion process of embedded steel in the supplementary cementitious materials (including coal fly ash, silica fume, and volcanic ash, *etc*.) modified Portland cement[24-29]. Structural differences caused by multiple factors will also have a greater impact on the erosion resistance of cement[30-32]. Recently, the interest on innovative binders based on calcium aluminate cement (CAC) has increased, which is mainly related to its corrosion resistance[33-38].

Although there is a problem of strength retraction owing to the phase conversion from hexagonal calcium aluminate hydrates ($CAH_{10}$, $C_2AH_8$) to the cubic one ($C_3AH_6$), studies showed the excellent corrosion resistance of CAC in severe environments, especially for marine engineering[33,39]. Many CAC structures continue to provide satisfactory service after several decades[40,41]. And binary or ternary systems composed of CAC and Portland cement or pozzolanic materials also exhibited better resistance to chloride attack[33,42-46]. This offers possible reentry of CAC to the family of high-performance building materials. Due to the low alkalinity of CAC concrete, it could have adverse effects on the corrosion protection to the steel reinforcement, but CAC enhances its chloride binding capacity to form Friedel's salt because of its high content of $Al_2O_3$[34,36,47], which is conducive to the resistance to chloride-induced corrosion of steel reinforcement. Therefore, the chloride corrosion resistance of CAC binders in relation to the durability of reinforced concrete structures is still with mysteries, especially regarding to the electrochemical corrosion behavior of steel reinforcement in CAC-based concrete[33,38,39].

To further clarify the electrochemical corrosion behavior of the steel reinforcement in CAC, the corrosion potential, electrochemical impedance spectroscopy, and linear polarization parameters were measured to identify the corrosion process of the reinforced CAC mortar immersed in different concentrations of chloride solution.

# 2 Experimental

## 2.1 Raw materials

CAC used in this study was supplied by Kerneos Aluminate Technologies (China) with grade CA50. Its chemical composition measured by XRF is given in Table 1. The main mineral composition of CAC tested by QXRD is summarized in Table 2. Q235 ordinary round steel bar was used as the embedded steel, and its tensile strength was 412 MPa. The chemical composition of the steel bar is shown in Table 3. Sand and deionized water were also employed. The particle size distribution of sand is listed in Table 4. Chemically pure NaCl reagent was utilized as the chloride source.

**Table 1 Chemical composition of CAC/wt%**

| MgO | $Al_2O_3$ | $SiO_2$ | $P_2O_5$ | $SO_3$ | Cl | $K_2O$ | CaO | $TiO_2$ | MnO | $Fe_2O_3$ |
|---|---|---|---|---|---|---|---|---|---|---|
| 0.46 | 48.45 | 7.33 | 0.15 | 0.46 | 0.01 | 0.45 | 37.87 | 2.52 | 0.04 | 1.90 |

**Table 2 Mineralogical composition of CAC/wt%**

| CA | $CA_2$ | $C_2AS$ | CT |
|---|---|---|---|
| 51.12 | 4.31 | 35.15 | 4.86 |

**Table 3 Chemical composition of the steel bar/wt%**

| C | Si | Mn | P | S | Ni | Cr | Cu | Fe |
|---|---|---|---|---|---|---|---|---|
| 0.14 | 0.18 | 0.33 | 0.017 | 0.004 | 0.01 | 0.01 | 0.01 | 99 |

**Table 4 Particle size distribution of sand**

| Side length of square hole/mm | Range of cumulative sieve surplus/% | Actual cumulative sieve surplus/% |
|---|---|---|
| 2.00 | 0 | 0.00 |
| 1.60 | 7±5 | 8.15 |
| 1.00 | 33±5 | 33.24 |
| 0.50 | 67±5 | 66.65 |
| 0.16 | 87±5 | 87.87 |
| 0.08 | 99±5 | 99.56 |

## 2.2 Specimen preparation

For specimen preparation, in order to accelerate the corrosion process and shorten the test period, the water to cement ratio was fixed at 0.6. And the cement to sand ratio was 1:3. Before molding, the surface of the steel bars was polished step by step with sandpaper

of 400#, 800#, 1 200#, and 2 000#, until the bright silvery-white metallic luster was emitted, then the steel bars were ultrasonically cleaned with absolute ethanol and blown dry with a cold air blower. One end of the steel bars (with a diameter of 10 mm and height of 30 mm) was welded with copper wires and then the upper and lower ends of the steel bars were coated with epoxy. The cylindrical side of each steel bar was as the working surface with an area of 9.425 $cm^2$. Prior to being embedded in the concrete, the steel bars were immersed in strong alkaline solution for 8 days to promote passivation. After that, the reinforced cylindrical specimens (with a diameter of 70 mm and a height of 35 mm) were prepared to study the corrosion behavior of steel bars embedded in CAC mortars. All specimens were cured in an environment of 20±2.0 ℃ and relative humidity of 98±2.0% for 8 days and then the two round ends of the specimens were also coated with epoxy to ensure that only the cylindrical sides of the specimens were directly in contact with the chloride salt solution in a subsequent corrosion test.

## 2.3 Chloride corrosion

The above-mentioned specimens after pre-cured for 8 days were continuously immersed in different concentrations of chloride salt solutions at 20±2.0 ℃, 3 specimens were chosen as a set, as shown in Table 5, and every month the solutions were changed. The volume ratio of each set of specimens to the solution was 1:20. Electrochemical tests were carried out on the immersed specimens regularly.

**Table 5 Grouping of chloride corrosion test**

| Designation | Thickness of mortar layer/mm | Solution/wt% |
|---|---|---|
| W | 30 | deionized water |
| MRI | 30 | 3% NaCl |
| MRII | 30 | 9% NaCl |
| MRIII | 30 | 15% NaCl |

## 2.4 Electrochemical test

The classic three-electrode system was utilized in the electrochemical test. Each reinforced CAC specimen acted as a working electrode. A saturated calomel electrode (model number 232, made by INESA Scientific Instrument Co., Ltd) and a platinum electrode (model number 213, ibid.) were selected as the reference electrode and the counter electrode respectively. The 3 electrodes were connected with a CHI 660E electrochemical workstation (manufactured by CH Instruments, Inc.) and a computer to form a testing system. All test results derived from the average of 3 specimens in each set.

After connecting the circuit, the corrosion potential was measured firstly by open circuit potential (OCP) test procedure of the electrochemical workstation. The corrosion potential of the specimen was the potential difference between the specimen and the saturated calomel electrode. If the OCP did not exceed ±2 mV within 5 min, the corrosion system was considered to be stable, and the final value was identified as the corrosion potential.

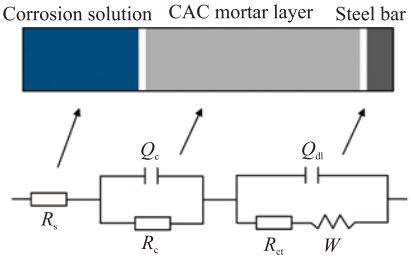


Fig.1 Equivalent circuit model for fitting EIS data

The electrochemical impedance spectroscopy (EIS) test was performed after the corrosion potential testing. It was obtained under a frequency range from $10^5$ Hz to $10^{-2}$ Hz. In order to quantitatively analyze the microstructure of CAC mortar and the electrochemical characteristics of the steel reinforcement during the corrosion process, the ZSimpWin software program was used to provide the equivalent circuit model for analyzing the EIS data. After comprehensively comparing the fitting effects of various classical equivalent circuit models[27,48-53], the model $R_s(Q_cR_c)(Q_{dl}(R_{ct}W))$ was used to fit the impedance spectroscopy of the reinforced CAC mortar for chloride ion attack (shown in Fig.1). In the proposed model, $R_s$ is the resistivity of the chloride salt solution, $Q_c$ is the capacitance of the interface between the specimen and the salt solution, $R_c$ is the resistivity of the CAC mortar layer, $Q_{dl}$ is the double-layer capacitance between the steel bar and the mortar layer, $R_{ct}$ is the resistivity of the charge transfer on the surface of steel bar, $W$ is the Warburg resistivity of the charge diffusion.

The corrosion current density can quantitatively characterize the corrosion degree of the reinforcement, but it is difficult to be measured directly. It is generally determined according to the Stern-Geary formula[36,39].

$$i_{corr} = B/R_p \tag{6}$$

where $B$ is given by

$$B = \beta_a\beta_c/2.3(\beta_a+\beta_c) \tag{7}$$

$\beta_a$ and $\beta_c$ are the Tafel slopes of the cathodic and

anodic processes respectively. But for the corrosion process of the reinforcement in concrete, $B$ can be considered as a constant to calculate other electrochemical parameters[36,39]. So the higher the polarization resistivity $R_p$, the lower the corrosion current density $i_{corr}$ and the slower the corrosion rate. Therefore, the polarization resistivity $R_p$ is an important parameter to study the corrosion dynamics of the steel reinforcement. In order to get it, the linear polarization curves were obtained using the linear sweep voltammetry (LSV) method, and the AC voltage amplitude was 10 mV, scanning rate was 0.5 mV/s. Then the polarization results were approximated to a straight line, and the slope of the straight line is the reciprocal of $R_p$.

# 3 Results and discussion

## 3.1 Corrosion potential of steel bar in CAC mortar

The corrosion potential of reinforced CAC mortar electrodes immersed in different concentrations of NaCl solutions are shown in Fig.2. The initial corrosion potential of the control (W set) is −260 mV, and it is positively shifted around 60 mV within 28 days. Therefore, the passive film on the rebar surface is stable and strengthened during this period, and CAC mortar layer ensures the reinforcement is in a passive state. At 40 days, the corrosion potential decreases to −260 mV again, and the passive film on the rebar surface gradually becomes thinner from 28 to 40 days. When the immersion age increases to 60 days, the corrosion potential reaches −590 mV, and further decreases with the extension of age. It shows that the passive film is destroyed and the corrosion degree is gradually deepened. For specimens immersed in 3% NaCl solution (MRI set), the corrosion potential is gradually reduced with age, which suggests that the passive film on the surface of reinforcement is not stable under the chloride corrosion environment. It decreases slightly within 28 days, and then dramatically drops by 320 mV at 40 days, illustrating that the passive film is exhausted and the reinforcement is corroded. With further increase of age, the corrosion potential continues to decrease and the corrosion degree is aggravated. In contrast, the corrosion potential of specimens immersed in 9% NaCl solution (the MRII set) and 15% NaCl solution (MRIII set) do not change obviously within 120 days. This finding indicates that CAC mortar plays a prominent role in protecting the inner steel bar under high concentrations of chloride corrosion.

Comparing the corrosion potential change of four sets of reinforced CAC mortar electrodes, the corrosion potential of the MRI set first suddenly drops (the passive film is destroyed firstly), and followed by the W set. Different from the above two sets of specimens, the MRII and MRIII sets do not undergo significant corrosion damage within 120 days. Considering the corrosion of the MRI set, it may result from that with a lower concentration of $Cl^-$ intruding into CAC matrix, the reaction between calcium aluminate hydrates and $Cl^-$ to form Friedel's salt is slow in the short term[54,55]. And few Friedel's salt can not well refine the pore structure of CAC mortar to resist further ingress of external $Cl^-$. The corrosion of the reference (W set) depends mainly on the low compactness of CAC mortar prepared by high water to cement ratio, and thus the diffusion of oxygen becomes the corrosion controlling factor[42]. As for the MRII and MRIII sets in higher concentration of NaCl solutions, NaCl is much easier to crystallize and adhere to the surface of the specimen, which acts as a barrier to hinder the further ingress of external $Cl^-$. Additionally, CAC mortar combines with $Cl^-$ to generate massive Friedel's salt, thereby refining the pore structure and delaying the further ingress of chloride from the outside[39,56]. And the combination process of $Cl^-$ and hydration products is accompanied by the increase of free $OH^-$ in the pore solution, which enhances the alkalinity of CAC pore solution, also achieving a better protection of the inner steel bar[44].

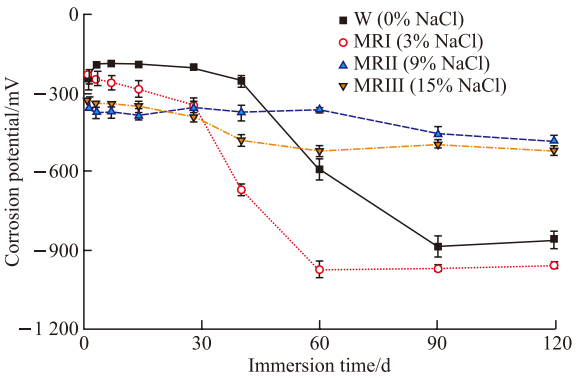


Fig.2 Corrosion potential of reinforced CAC mortar electrodes

## 3.2 Electrochemical impedance spectroscopy

The Nyquist curves of reinforced CAC mortar electrodes are given in Fig.3. All Nyquist curves appear as two interconnected arcs at different corrosion ages. The impedance arcs in the high-frequency zone (the left half curves in Fig.3 (a-d)) reflect the microstructure of CAC mortar layer, and the impedance arcs in the low-frequency zone (the right half curves in Fig.3 (a-d)) show the electrochemical properties of the passive film.

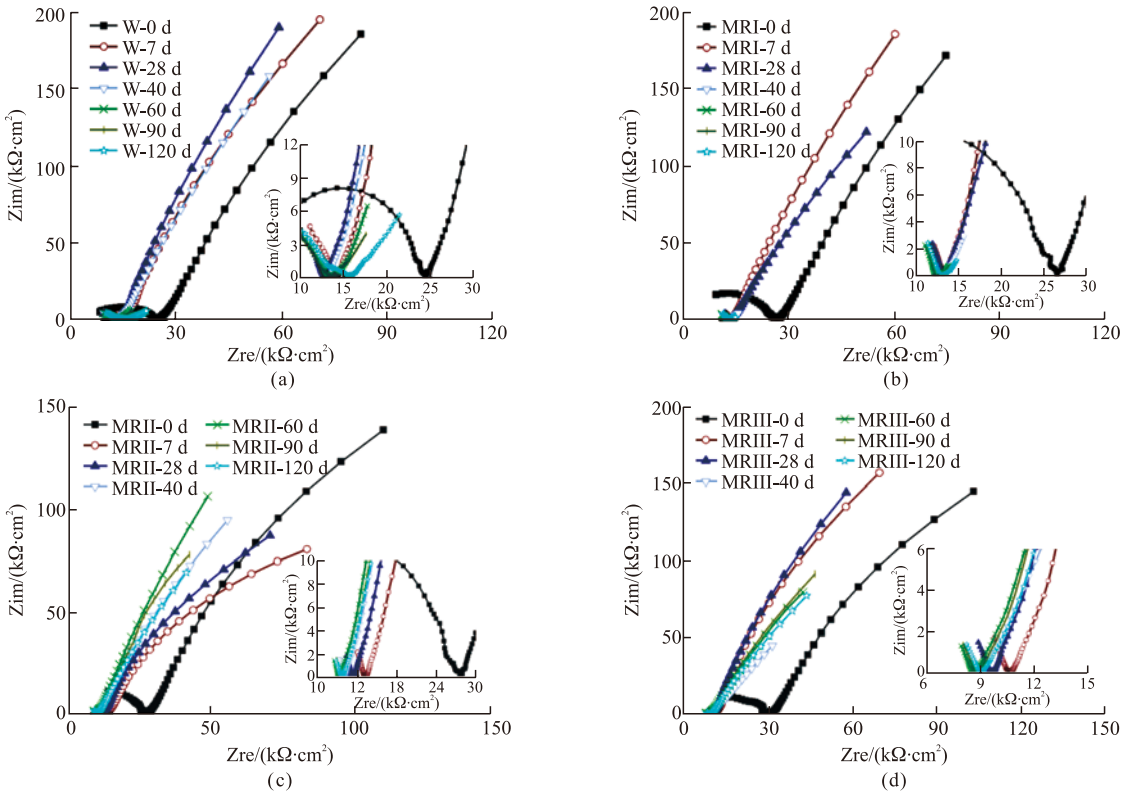


Fig.3 Nyquist curves of reinforced CAC mortar electrodes: (a) W set; (b) MRI set; (c) MRII set; (d) MRIII set

As shown in Fig.3 (a), when the specimens in W set are immersed for 0, 7, 28, and 40 days, its impedance arcs in the low-frequency region are close to straight lines with their slopes more than 1, indicating that the impedance arcs have large diameters. According to the typical characteristics of impedance arcs in the low-frequency region for passive steel reinforcement[49], it can be determined that the passive film is stable to keep the inner reinforcement in a relatively good passive state during the immersion time. It is consistent with the change in its corrosion potential. After 60 days, the diameters of the impedance arcs in the low-frequency region decrease sharply. It indicates the collapse of the resistivity of CAC mortar layer and the charge transfer resistivity of the steel bar.

For the EIS results of the MRI set (Fig.3 (b)), the diameters of the impedance arcs in the low-frequency zone are large within 28 days, meaning that the reinforcing steel is in a passive state. However, after 40 days, the Nyquist curves in both low and high frequency regions become flattened arcs, and the diameters of them decrease gradually with an increase of age. This can be mainly because the concentration of $Cl^-$ on the surface of steel reinforcement reaches a certain threshold with increasing immersion time[6], which results in the destruction of the passive film and a sharp decrease of the resistivity of steel reinforcement. Compared with the EIS data of W set, the diameters of the impedance arcs in the low-frequency zone are smaller, indicating that the initial corrosion time of the MRI set is advanced, which is consistent with the above corrosion potential test results.

The Nyquist curves of the MRII set are depicted in Fig.3(c). It can be seen that the diameters of the impedance arcs in the low-frequency zone decrease slightly within 7 days, suggesting the passive film on the surface of steel reinforcement is unstable at the early age. It lies in that the concentration of $Cl^-$ infiltrated into the CAC mortar is too low to reach the concentration threshold for Friedel's salt crystallization[39,54], and the protection ability of CAC mortar to the reinforcement is weakened. When the immersion time increases to 40 and 60 days, the diameters of the impedance arcs increase slightly, owing to more $Cl^-$ is combined to form Friedel's salt with the increase of age, which improves the protection ability of CAC mortar to reinforcement[56]. With the corrosion age further extending to 120 days, the change of impedance arcs is not obvious.

Fig.3(d) shows the Nyquist curves of the MRIII set. Within 120 days, although the diameters of the impedance arcs in the low-frequency region decrease with

age, this change is not obvious. Therefore, the failure rate of the passive film is slow, which mainly benefits from the formation of Friedel's salt[36,56]. Compared with the W and MRI set, the corrosion degree of steel bars in MRIII set is still lower even after the immersion in a higher concentration of NaCl solution for 120 days. CAC mortar plays a significant role in protecting the inner steel bar in such a severe chlorine-rich environment.

### 3.3 Fitting calculation of electrochemical parameters

The Nyquist curves enable the tracing of chloride migration in the cement mortar[49]. In order to quantitatively analyze the effect of chloride concentration on the corrosion process of reinforced CAC mortar, it is necessary to determine the electrical parameters of the equivalent circuit components. The resistivity of CAC mortar ($R_c$) obtained by fitting the Nyquist curves data is given in Fig.4, and the resistivity of charge transfer ($R_{ct}$) is listed in Table 6.

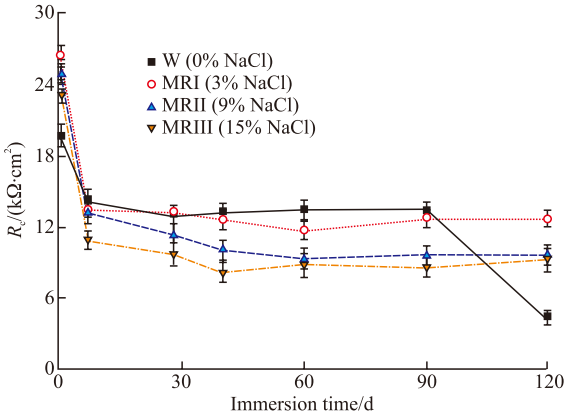


Fig.4 Variation of the resistivity of CAC mortar ($R_c$) with immersion time

$R_c$ reflects the microstructure of CAC mortar layer. With the increasing immersion time, the $R_c$ of all specimens shows a downward trend. Especially within 7 days, the value of $R_c$ decreases the most, which is mainly due to the water absorption and saturation process of the mortar layer. Moreover, the higher the concentration of salt solution, the greater the decrease of $R_c$ during this period. For example, the $R_c$ of the W set decreases by 5.42 kΩ·cm$^2$ within 7 days, while that of the MRIII set decreases by 12.37 kΩ·cm$^2$, almost half of the initial value. When the immersion time increases from 28 days to 90 days, the downward trend of $R_c$ values of all specimens is gradually slowing down. This finding confirms that the compact state of CAC mortar in each group is relatively stable and not obviously influenced by chloride corrosion. At 120 days, the $R_c$ of W set decreases sharply, from 13.29 kΩ·cm$^2$ (at 90 days) to 4.34 kΩ·cm$^2$. It may be owing to the more prominent phase conversion of hydrates with the increase age[33,57]. While the $R_c$ of specimens immersed in NaCl solution (MRI, MRII, and MRIII set) does not change significantly at 120 days. It results from that the formation of Friedel's salt inhibits the phase conversion of the calcium aluminate hydrates and also further fines the pore structure of CAC mortar[36,53].

**Table 6 The resistivity of charge transfer ($R_{ct}$) changing with immersion time/kΩ·cm$^2$**

| Immersion time/d | W | MRI | MRII | MRIII |
|---|---|---|---|---|
| 0 | $4.41\times10^{11}$ | $1.02\times10^{12}$ | $8.57\times10^{9}$ | $8.32\times10^{9}$ |
| 7 | $1.42\times10^{12}$ | $1.34\times10^{11}$ | $2.61\times10^{9}$ | $2.40\times10^{9}$ |
| 28 | $4.84\times10^{13}$ | $1.96\times10^{8}$ | $4.32\times10^{8}$ | $1.24\times10^{8}$ |
| 40 | $2.42\times10^{9}$ | 26.41 | $1.00\times10^{8}$ | $8.83\times10^{7}$ |
| 60 | 33.42 | 12.08 | $5.51\times10^{8}$ | $5.17\times10^{6}$ |
| 90 | 13.29 | 12.68 | $9.71\times10^{7}$ | $8.96\times10^{7}$ |
| 120 | 11.43 | 12.63 | $9.75\times10^{6}$ | $2.41\times10^{5}$ |

The variation of $R_{ct}$ with age directly reflects the de-passivation and corrosion process of the reinforcement. As listed in Table 6, the $R_{ct}$ of the W set gradually increases within 28 days, and there is a stable passive film on the surface of the inner steel bar. After that, the value of $R_{ct}$ decreases slightly at 40 days. When the immersion time increases to 60 days, the value of $R_{ct}$ decreases by 8 orders of magnitude compared with that at 40 days. It illustrates that the passive film is destroyed and the passive state of reinforcement changes to the activated state. After 60 days, the $R_{ct}$ of W set continues to decrease and the corrosion process of steel reinforcement is accelerated. For the MRI group, the $R_{ct}$ gradually decreases with age, and it changes sharply at 40 days, which is 7 orders of magnitude lower than that at 28 days, mainly due to the failure of the passive film. At 60 days, the $R_{ct}$ of the MRI set further decreases, but after that, it changes little with the increase of age and the corrosion rate slows down. It is consistent with the corrosion potential test results. The $R_{ct}$ values of the MRII and MRIII sets also decrease with age. But it changes less within 120 days than that of W and MRI set, only decreasing by 3 to 4 orders of magnitude and does not drop suddenly. It further confirms that even under a higher concentration of chloride corrosion, CAC mortar can prominently weaken the chloride attack on the reinforcing steel.

### 3.4 Linear polarization

For further quantitative analysis, the linear fitting results are summarized in Table 7. It can be seen that

before the corrosion (0 d), the polarization resistivity $R_p$ of each set is around 12-23 kΩ·cm$^2$, and the linear correlation coefficient $R^2$ ranges from 0.5 to 0.7. There is a complete passive film on the surface of reinforcement. With the proceeding of immersion, the changing trend of $R_p$ in four sets varies from each other.

**Table 7 Linear polarization fitting results of the reinforced CAC mortar electrodes immersed in different concentrations of NaCl solutions**

| Designation | Fitting term | Immersion time/d | | | | | | |
|---|---|---|---|---|---|---|---|---|
| | | 0 | 7 | 28 | 40 | 60 | 90 | 120 |
| W | $R_p$ /(kΩ·cm$^2$) | 22.7 | 32.2 | 32.6 | 22.5 | 1.79 | 1.60 | 2.08 |
| | $R^2$ | 0.545 | 0.563 | 0.521 | 0.523 | 0.977 | 0.992 | 0.980 |
| MRI | $R_p$ /(kΩ·cm$^2$) | 12.4 | 14.0 | 8.41 | 1.57 | 1.43 | 1.49 | 1.50 |
| | $R^2$ | 0.720 | 0.637 | 0.694 | 0.993 | 0.999 | 0.998 | 0.998 |
| MRII | $R_p$ /(kΩ·cm$^2$) | 16.1 | 11.0 | 11.3 | 11.2 | 13.0 | 8.91 | 6.92 |
| | $R^2$ | 0.691 | 0.779 | 0.742 | 0.640 | 0.574 | 0.570 | 0.613 |
| MRIII | $R_p$ /(kΩ·cm$^2$) | 16.0 | 22.1 | 19.4 | 4.32 | 8.30 | 9.92 | 7.95 |
| | $R^2$ | 0.646 | 0.563 | 0.534 | 0.668 | 0.582 | 0.569 | 0.590 |

The $R_p$ of the W set increases first and then decreases with age. At 28 days, it increases by 10 kΩ·cm$^2$ compared with that at 0 d, indicating that the passive film is strengthened. When the age increases to 60 days, the $R_p$ of the W set is reduced by an order of magnitude and the linear correlation coefficient $R^2$ reaches 0.977. This finding explains that the corrosion current density increases to about 10 times at 40 days. With respect to the MRI set, its polarization resistivity $R_p$ increases within 7 days. But after 28 days, it decreases with the extension of immersion time. The passive film gradually disappears owing to the chloride corrosion. When the immersion time increases to 40 days, the $R_p$ of the MRI set drops to 1.57 kΩ·cm$^2$, and the linear correlation coefficient $R^2$ is close to 1. There is a good linear relationship between the current density and potential at 40 days. It illustrates that the concentration of free $Cl^-$ near the steel surface has accumulated to a certain threshold to corrode the embedded steel[6,58]. Compared with the reference (W set), the initial corrosion time of the MRI set is earlier. The $R_p$ of the MRII set changes slightly and the linear correlation coefficient $R^2$ is about 0.5-0.7 within 120 days. There is a relatively slow corrosion process of inner reinforcement in MRII set, which may benefit from the binding effect of CAC mortar layer on chloride ions[39]. Additionally, the variation of $R_p$ and $R^2$ in the MRIII set is similar to that of the MRII set.

Overall, compared with the control, the corrosion process of the MRI set immersed in the low concentration of NaCl solution is accelerated, while it is delayed for the MRII and MRIII groups immersed in a high concentration of NaCl solution. CAC mortar exhibits excellent performance against chloride attack in the high concentration of chloride salt solution to protect steel reinforcement.

### 3.5 Macroscopic corrosion morphology

The steel reinforcements in CAC mortars immersed in different concentrations of chlorides for 120 d are given in Fig.5. It is evident that all steel reinforcements in the W set are passive, due to its relatively porous structure caused by the large water to cement ratio (0.6). Also, the phase transition of CAC hydrates has a negative effect on its porous structure, which makes it easier to be exposed to water and oxygen and thus leads to accelerated corrosion. Compared with the control, a larger amount of rust can be observed in MRI set, while relatively few pitting pits in MRII and MRIII sets. The corrosion of steel rebar in low concentration of NaCl solution is accelerated while being delayed in high concentration ones. The result is consistent with the results of electrochemical tests, indicating that the chloride binding ability of CAC in low concentration of NaCl solution is weak, with most chloride remaining free, resulting in a poor performance against chloride attack.

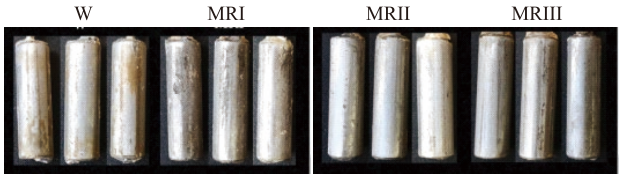


Fig.5 Macroscopic corrosion morphology of steel reinforcement in CAC mortar at 120 d

## 4 Conclusions

In this work, the electrochemical corrosion behavior of steel reinforcement in CAC mortar has been evaluated considering the effect of external chloride concentration and electrochemical testing technologies. Based on the experimental results, the following conclusions can be obtained:

a) The corrosion potential, electrochemical impedance spectroscopy assisting with an equivalent circuit model, and the linear polarization have good consistency in describing the chloride corrosion process of the reinforced CAC mortars.

b) The corrosion process of the embedded steel in CAC mortar is accelerated by low concentration chloride corrosion, while initial corrosion time is delayed when the reinforced CAC mortars are immersed in high

concentrations of NaCl solution. This phenomenon may partially relate to the chemical bonding and adsorption of CAC paste with the chloride ions.

c) The reference (W group) shows obvious de-passivation and corrosion state at 60 days. Compared with the reference, the reinforcement in the CAC mortar immersed in 3% NaCl solution (MRI set) is already in a corrosion-activated state at 40 days and is more severely corroded at 120 days. However, the embedded steel in the CAC mortar immersed in 9% (MRII set) and 15% NaCl (MRIII set) solutions are less corroded within 120 days, with slight pitting.

## References


[1] Bertolini L, Elsener B, Pedeferri P, *et al*. Corrosion of Steel in Concrete: Prevention, Diagnosis, Repair[J]. *Wiley-VCH Verlag GmbH & Co. KGaA*., 2013, 49(1 065): 4 113-4 133

[2] De Weerdt K , Plusquellec G , Belda Revert A, *et al*. Effect of Carbonation on the Pore Solution of Mortar[J]. *Cement Concrete Res*., 2019, 118: 38-56

[3] Vollpracht A, Lothenbach B, Snellings R, *et al*. The Pore Solution of Blended Cements: a Review[J]. *Mater. Struct*., 2016, 49(8): 3 341-3 367

[4] Behnood A, Tittelboom KV, Belie ND. Methods for Measuring pH in Concrete: A Review[J]. *Constr. Build. Mater*., 2016, 105: 176-188

[5] Vélez W, Matta F, Ziehl P. Electrochemical Characterization of Early Corrosion in Prestressed Concrete Exposed to Salt Water[J]. *Mater. Struct.*, 2016, 49(1): 507-520

[6] Cao Y, Gehlen C, Angst U, *et al*. Critical Chloride Content in Reinforced Concrete - An Updated Review Considering Chinese Experience[J]. *Cement Concrete Res*., 2019, 117: 58-68

[7] Castellote M, Fernandez L, Andrade C, *et al*. Chemical Changes and Phase Analysis of OPC Pastes Carbonated at Different $CO_2$ Concentrations[J]. *Mater. Struct.*, 2009, 42(4):515-525

[8] Yuan Y, Shen J. Comparison of Concrete Carbonation Process under Natural Condition and High $CO_2$ Concentration Environments[J]. *J. Wuhan Univ. Technol. -Mater. Sci. Ed.*, 2010, 25: 515-522

[9] Houst YF, Wittmann FH. Influence of Porosity and Water Content on the Diffusivity of $CO_2$ and $O_2$ through Hydrated Cement Paste[J]. *Cement Concrete Res.*, 1994, 24(6): 1 165-1 176

[10] Ngala VT. Effects of Carbonation on Pore Structure and Diffusional Properties of Pydrated Cement Pastes[J]. *Cement Concrete Res.*, 1997, 27: 995-1 007

[11] Yohai L, Schreiner W, Valcarce MB, *et al*. Inhibiting Steel Corrosion in Simulated Concrete with Low Phosphate to Chloride Ratios[J]. *J. Electrochem. Soc.*, 2016, 163(13): 729-737

[12] Figueira RB, Sadovski A, Melo AP, *et al*. Chloride Threshold Value to Initiate Reinforcement Corrosion in Simulated Concrete Pore Solutions: The Influence of Surface Finishing and pH[J]. *Constr. Build. Mater*., 2017, 141: 183-200

[13] Marcotte TD, Hansson CM. Corrosion Products that Form on Steel within Cement Paste[J]. *Mater. Struct.*, 2007, 40(3): 325-340

[14] Dhouibi L, Triki E, Raharinaivo A. The Application of Electrochemical Impedance Spectroscopy to Determine the Long-term Effectiveness of Corrosion Inhibitors for Steel in Concrete[J]. *Cem. Concr. Compos.*, 2002, 24(1): 35-43

[15] Soeylev TA, Richardson MG. Corrosion Inhibitors for Steel in Concrete: State-of-the-Art Report[J]. *Constr. Build. Mater*., 2008, 22(4): 609-622

[16] Trépanier SM, Hope BB, Hansson CM. Corrosion Inhibitors in Concrete[J]. *Cement Concrete Res.*, 2001, 31(5): 713-718

[17] Zheng H, Li W, Ma F, *et al*. The Effect of a Surface-applied Corrosion Inhibitor on the Durability of Concrete[J]. *Constr. Build. Mater.*, 2012, 37: 36-40

[18] Shihao MA, Weihua LI, Zheng H, *et al*. Research Progress of Anti-corrosion Mechanism and Performance Evaluation of Corrosion Inhibitor for Steel Bar[J]. *Corrosion & Protection*, 2017, 38: 963

[19] Ngala VT, Page CL, Page MM. Corrosion Inhibitor Systems for Remedial Treatment of Reinforced Concrete. Part 1: Calcium Nitrite[J]. *Corros. Sci*., 2002, 44(9): 2 073-2 087

[20] Ngala VT, Page CL, Page MM. Corrosion Inhibitor Systems for Remedial Treatment of Reinforced Concrete. Part 2: Sodium Monofluorophosphate[J]. *Corros. Sci*., 2003, 45(7): 1 523-1 537

[21] Morris W, Vico A, Vazquez M, Sanchez SR. Corrosion of Reinforcing Steel Evaluated by Means of Concrete Resistivity Measurements[J]. *Corros. Sci.*, 2002, 44: 81

[22] Yuan CF, Niu DT. Chloride Ion Diffusion Model of the Concrete under Multiple Factors[J]. *Advanced Science Letters*, 2012, 14(1): 332-335

[23] Carsana M , Canonico F , Bertolini L . Corrosion Resistance of Steel Embedded in Sulfoaluminate-based Binders[J]. *Concr. Compos.*, 2018, 88: 211

[24] Kou S, Poon CS. Compressive Strength, Pore Size Distribution and Chloride-ion Penetration of Recycled Aggregate Concrete Incorporating Class-F Fly Ash[J]. *J. Wuhan Univ. Technol. -Mater. Sci. Ed.*, 2006, 21(04): 130-136

[25] Mccarthy MJ, Tittle P, Dhir RK. Corrosion of Reinforcement in Concrete Containing Wet-stored Fly Ash[J]. *Cem. Concr. Compo.,* 2019, 71: 102

[26] Heniegal AM, Amin M, Youssef H. Effect of Silica Fume and Steel Slag Coarse Aggregate on the Corrosion Resistance of Steel Bars[J]. *Constr. Build. Mater.*, 2017, 155: 846-851

[27] Monticelli C, Natali ME, Balbo A, *et al*. Corrosion Behavior of Steel in Alkali-activated Fly Ash Mortars in the Light of Their Microstructural, Mechanical and Chemical Characterization[J]. *Cement Concrete Res.*, 2016, 80: 60-68

[28] Lachemi M, Hossain K, Lambros V, *et al*. Self-consolidating Concrete Incorporating New Viscosity Modifying Admixtures[J]. *Cement Concrete Res.*, 2004, 34(6): 917-926

[29] Kwasi, Osafo, Ampadu, *et al*. Chloride Ingress and Steel Corrosion in Cement Mortars Incorporating Low-quality Fly Ashes[J]. *Cement Concrete Res.*, 2002, 32(6): 893-901

[30] Wu K, Hu Y, Zhang L, *et al*. Promoting the Sustainable Fabrication

of Bricks from Municipal Sewage Sludge Through Modifying Calcination: Microstructure and Performance Characterization [J]. *Constr. Build. Mater.*, 2022, 324: 126 401

[31] Wang Z, Chen Y, Xu L, *et al*. Insight into the Local C-S-H Structure and Its Evolution Mechanism Controlled by Curing Regime and Ca/Si Ratio[J]. *Constr. Build. Mater.*, 2022, 333: 127 388

[32] Zhou Y, Wang Z, Zhu Z, *et al*. Time-varying Structure Evolution and Mechanism Analysis of Alite Particles Hydrated in Restricted Space[J]. *Constr. Build. Mater.*, 2022, 341: 127 829

[33] Ann K, Cho CG. Corrosion Resistance of Calcium Aluminate Cement Concrete Exposed to a Chloride Environment[J]. *Materials*, 2014, 7(2): 887-898

[34] Argiz C, Angel Sanjuan M, Castro Borges P, *et al*. Modeling of Corrosion Rate and Resistivity of Steel Reinforcement of Calcium Aluminate Cement Mortar[J]. *Adv. Civ. Eng.*, 2018(PT.1): 1-9

[35] Ukrainczyk N, Vrbos N, Šipušić J. Influence of Metal Chloride Salts on Calcium Aluminate Cement Hydration[J]. *Adv. Cem. Res.*, 2012, 2012(5): 249-262

[36] Ann KY, Kim TS, Kim JH, *et al*. The Resistance of High Alumina Cement Against Corrosion of Steel in Concrete[J]. *Constr. Build. Mater.*, 2010, 24(8): 1 502-1 510

[37] Sanjuan MA. Formation of Chloroaluminates in Calcium Aluminate Cements Cured at High Temperatures and Exposed to Chloride Solutions[J]. *J. Mater. Sci.*, 1997, 32(23): 6 207-6 213

[38] Sanjuán MA. Effect of Curing Temperature on Corrosion of Steel Bars Embedded in Calcium Aluminate Mortars Exposed to Chloride Solutions[J]. *Corros. Sci.*, 1998, 41(2): 335-350

[39] Macias A, Kindness A, Glasser FP. Corrosion Behaviour of Steel in High Alumina Cement Mortar Cured at 5, 25 and 55 ℃: Chemical and Physical Factors[J]. *J. Mater. Sci.*, 1996, 31(9): 2 279-2 289

[40] Barnes P. Structure and Performance of Cements[J]. *Can. J. Civil Eng.*, 2002, 1: 226-231

[41] Bate, Cc S. *High Alumina Cement Concrete in Existing Building Superstructures*[M]. Garston: Building Research Establishment, 1984

[42] Li G, Zhang A, Song Z, *et al*. Ground Granulated Blast Furnace Slag Effect on the Durability of Ternary Cementitious System Exposed to Combined Attack of Chloride and Sulfate[J]. *Constr. Build. Mater.*, 2018, 158(15): 640-648

[43] Moradllo MK , Ley MT . Comparing Ion Diffusion in Alternative Cementitious Materials in Real Time by Using Non-destructive X-ray Imaging[J]. *Cem. Concr. Compos*., 2017, 82: 67-79

[44] Moffatt EG, Thomas MA. Performance of Rapid-repair Concrete in an Aggressive Marine Environment[J]. *Constr. Build. Mater.*, 2017, 132(1): 478-486

[45] Li G, Zhang A, Song Z, *et al*. Study on the Resistance to Seawater Corrosion of the Cementitious Systems Containing Ordinary Portland Cement or/and Calcium Aluminate Cement[J]. *Constr. Build. Mater.*, 2017, 157: 852-859

[46] Jin SH, Yang HJ, Hwang JP, *et al*. Corrosion Behaviour of Steel in CAC-mixed Concrete Containing Different Concentrations of Chloride[J]. *Constr. Build. Mater.*, 2016, 110(1): 227-234

[47] Goñi S, Gaztañaga MT, Sagrera JL, *et al*. The Influence of NaCl on the Reactivity of High Alumina Cement in Water: Pore-solution and Solid Phase Characterization[J]. *J. Mate. Res.*, 1994, 9(6): 1 533-1 539

[48] Hoshi Y, Hasegawa C, Okamoto T, *et al*. Electrochemical Impedance Analysis of Corrosion of Reinforcing Bars in Concrete[J]. *Electrochemistry,* 2019, 87(1): 78-83

[49] Dong BQ, Wu YS, Teng XJ, *et al*. Investigation of the $Cl^-$ Migration Behavior of Cement Materials Blended with Fly Ash or/and Slag via the Electrochemical Impedance Spectroscopy Method[J]. *Constr. Build. Mater.*, 2019, 211: 261-70

[50] Nguyen W, Duncan JF, Devine TM, *et al*. Electrochemical Polarization and Impedance of Reinforced Concrete and Hybrid Fiber-reinforced Concrete under Cracked Matrix Conditions[J]. *Electrochim. Acta*, 2018; 271: 319-336

[51] Diaz B, Guitian B, Novoa XR, *et al*. The Effect of Long-term Atmospheric Aging and Temperature on the Electrochemical Behaviour of Steel Rebars in Mortar[J]. *Corros. Sci.*, 2018; 140: 143-150

[52] Pu Q, Jiang LH, Chu HQ, *et al*. Electrochemical Behavior of Steel Bar in Electrolytes: Influence of pH Value and Cations[J]. *J. Wuhan. Univ. Technol. -Mater. Sci*., 2011, 26(6): 1 133-1 136

[53] Sobhani J, Najimi M. Electrochemical Impedance Behavior and Transport Properties of Silica Fume Contained Concrete[J]. *Constr. Build. Mater.*, 2013; 47: 910-918

[54] Yuan Q, Shi C, De Schutter G, *et al*. Chloride Binding of Cement-based Materials Subjected to External Chloride Environment - A Review[J]. *Constr. Build. Mater.*, 2009;23(1): 1-13

[55] Rasheeduzzafar. Influence of Cement Composition on Concrete Durability[J]. *Aci. Mater. J.*, 1992, 89(6): 574-586

[56] Shao Y, Zhou M, Wang WX, *et al*. Identification of Chromate Binding Mechanisms in Friedel's Salt[J]. *Constr. Build. Mater.*, 2013, 48: 942-947

[57] Pacewska B, Nowacka M. Studies of Conversion Progress of Calcium Aluminate Cement Hydrates by Thermal Analysis Method[J]. *J. Therm. Anal. Calorim.*, 2014, 117(2): 653-660

[58] Ann KY, Song HW. Chloride Threshold Level for Corrosion of Steel in Concrete[J]. *Corros. Sci.*, 2007, 49(11): 4 113-4 114